

# Reaction of Gaseous Nitric Oxide with Nitric Acid on Silica Surfaces in the Presence of Water at Room Temperature

N. A. Saliba, H. Yang, and B. J. Finlayson-Pitts\*

Department of Chemistry, University of California, Irvine, Irvine, California 92697-2025

Received: June 19, 2001; In Final Form: August 27, 2001

The reaction of gaseous NO with HNO<sub>3</sub> on borosilicate glass in the presence of water was studied as a function of surface water coverage at 298 K and a total pressure of one atm in N<sub>2</sub>. The loss of gaseous NO and the formation of NO<sub>2</sub> were measured in a long path cell using FTIR. The glass walls of the cell provided the surface upon which the chemistry occurred. Water coverages on thin glass cover disks were determined in a separate apparatus by measuring the intensity of the infrared band of liquid water at 3400 cm<sup>-1</sup>. Approximately one monolayer was present on the surface at 20% RH and 12 monolayers at 100% RH. The rate of the reaction of NO with HNO<sub>3</sub> on the surface was the largest under conditions where approximately three surface monolayers of water were present on the surface. We propose a model for this reaction in which HNO<sub>3</sub>, added first to the dry cell, hydrogen-bonds to the silanol groups on the surface. The first step in the reaction is believed to be HNO<sub>3(surface)</sub> + NO<sub>(g)</sub> → HONO<sub>(surface)</sub> + NO<sub>2(g)</sub>. Subsequently, HONO on the surface reacts with HNO<sub>3</sub> to generate solvated N<sub>2</sub>O<sub>4</sub> as a product. Dissociation of N<sub>2</sub>O<sub>4</sub> generates NO<sub>2</sub> as the final gas phase product. This chemistry is potentially important in “renoxification” of the boundary layer of polluted urban atmospheres where silica surfaces are plentiful in particles, soils and building materials, as well as globally in the free troposphere where dust particles are present.

## I. Introduction

More than five decades of laboratory studies have shown that oxides of nitrogen react on surfaces in the presence of water. For example, Smith<sup>1</sup> noted during gas-phase studies of the reaction of NO with HNO<sub>3</sub> that there appeared to be a surface reaction dependent on water vapor. Such heterogeneous reactions may be potentially important in the atmosphere where oxides of nitrogen, present as air pollutants from combustion processes, are in contact with many surfaces in the form of suspended particles as soil, roads, buildings, and plants.

Despite the well-recognized occurrence of heterogeneous chemistry for the oxides of nitrogen, the kinetics and mechanisms of these reactions are not well understood. One difficulty arises in simultaneously measuring surface and gas-phase reaction species. However, recent infrared spectroscopic studies of heterogeneous hydrolysis of NO<sub>2</sub> on silica surfaces conducted by Grassian and co-workers<sup>2</sup> as well as by this laboratory,<sup>3</sup> showed that this well-known<sup>4–16</sup> reaction



produces N<sub>2</sub>O<sub>4</sub> as a key intermediate on the surface. HNO<sub>3</sub> was also observed spectroscopically on the surface as hypothesized in the previous studies<sup>4–16</sup> where only gas-phase measurements could be made, or nitrate ions measured in washings from the surface after reaction.

In subsequent studies, Mochida and Finlayson-Pitts<sup>17</sup> showed that gaseous NO reacts with HNO<sub>3</sub> on a “wet” porous glass to generate nitrogen dioxide as the major gas-phase product, along with small amounts of gas-phase HONO. Thus, the mechanism

of the reaction was proposed in two steps as described below



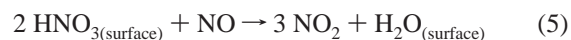
followed by subsequent reactions such as



or



The net reaction is



If all reactants and products are in the gas phase, reaction 2 is close to thermoneutral. However, the free energy change for reaction 2 with typical atmospheric concentrations of the reactants and products is negative, so that it has been proposed to be potentially feasible on surfaces in the atmosphere.<sup>18</sup>

Nitric acid is known to be readily taken up on a variety of surfaces, e.g., soil and its components such as silica.<sup>19–22</sup> Model studies<sup>23,24</sup> suggest that this uptake could impact NO<sub>x</sub> and O<sub>3</sub> in the troposphere. This process could also contribute to “renoxification” of the atmosphere and better reconcile field and modeling experiments,<sup>25,26</sup> especially if HNO<sub>3</sub> produces photochemically reactive species such as NO<sub>2</sub> and HONO. Thus, a discrepancy has been reported between the measured ratio of [HNO<sub>3</sub>]/[NO<sub>x</sub>] ≈ 5 in the free troposphere and the values of 15–100 predicted by models.<sup>25,26</sup> Although there are several hypotheses regarding the source of this discrepancy such as

\* To whom correspondence should be addressed: E-mail bfinlay@uci.edu. Phone: (949) 824-7670. Fax: (949) 824-3168.

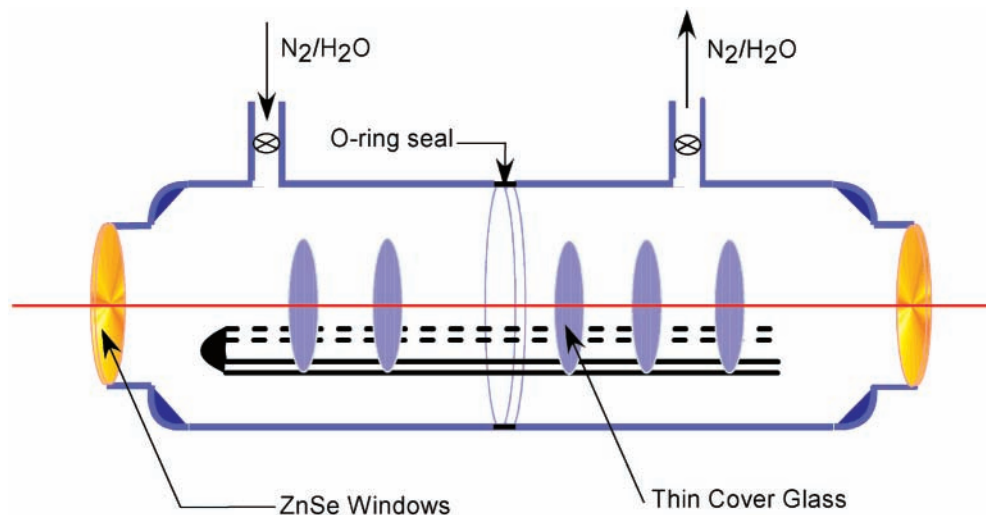


**Figure 1.** Cell used to measure water coverage on the borosilicate cover glass disks.

liquid-phase reactions of HCHO with HNO<sub>3</sub> in aerosols and cloud droplets, or reactions on soot,<sup>25–27</sup> the cause remains unknown.

To better understand the uptake and potential reactions of HNO<sub>3</sub> on surfaces, we have carried out further studies of the reaction of gaseous NO with HNO<sub>3</sub> on a smooth borosilicate glass surface as a function of varying amounts of surface-adsorbed water. The relationship between the gas phase water vapor concentration and the amount of water on the surface was established in a newly designed experimental apparatus using transmission FTIR and thin cover glass disks. These studies provide insight into the reactive forms of nitric acid on the surface and the reaction mechanism. The atmospheric implications are discussed.

## II. Experimental Section

**A. Measurements of Water Coverage on Thin Borosilicate Glass Disks.** The amount of liquid water adsorbed on thin cover glass disks at different relative humidities (RH) was determined by transmission infrared spectroscopy using the cell shown in Figure 1. The thin cover glass samples were thin Micro Cover Glasses (VWR Scientific, Inc.) with 0.13 to 0.17 mm thickness and 25 mm diameter. The cell, made of Pyrex glass, was 3.2 cm in diameter, 11 cm in length and capped with infrared-transmitting ZnSe windows. To increase the weak adsorbed H<sub>2</sub>O signal, five disks of cover glass were placed in thin slots along a U-shaped glass rod, giving a total of 10 glass surfaces for water uptake.

A mixture of water vapor in N<sub>2</sub> at various relative humidities was generated by diluting a 100% RH stream, obtained by bubbling N<sub>2</sub> through Nanopure water (Barnstead, 18 MΩ cm), with dry N<sub>2</sub>. The flow rates were controlled by calibrated Matheson TF 1050 flowmeters. Spectra were collected at 0.5 cm<sup>-1</sup> resolution with 1024 co-added scans and a total scan time of 14.5 min. A background spectrum was obtained after the cell and thin cover glass disks had been purged with dry N<sub>2</sub> for 24 h. Reference spectra of gas-phase water at different relative humidities were measured without the cover glass disks and subtracted before integration.

**B. Reaction of Gaseous NO with HNO<sub>3</sub> On a Borosilicate Glass Surface.** These experiments were performed in a long path infrared cell mounted vertically in the sample compartment of an FTIR spectrometer (Mattson, Cygnus) and equipped with an MCT detector. All experiments were carried out at 1 cm<sup>-1</sup>

resolution with 150 co-added scans and a total scan time of 3.9 min. The cell consists of a borosilicate glass cylinder (10 cm diameter × 91.4 cm length) and two stainless steel rods holding the mirrors (Al with a silicon monoxide protective coating) which are attached to two stainless steel plates at each end of the cell. To avoid reactions of the gases with the stainless steel, the metal surfaces were coated with halocarbon wax (Halocarbon Products Corp., Series 1500). The optical base path length was 0.8 m, with a total path length of 38.4 m. The long path cell was wrapped in a dark cloth to prevent photolysis of reactants and products.

Dry, gaseous HNO<sub>3</sub> obtained from the vapor above an HNO<sub>3</sub>/H<sub>2</sub>SO<sub>4</sub> mixture (1:2 v:v) was first admitted to the cell. HNO<sub>3</sub> was allowed to adsorb onto the cell walls over five minutes. The remaining gas-phase HNO<sub>3</sub> was then pumped out, and this conditioning/adsorbing process was repeated at least three times. An NO concentration of (0.65–40) × 10<sup>15</sup> molecule cm<sup>-3</sup> was then added into the cell as a mixture with N<sub>2</sub>. Initial relative humidities of 0, 20, 30, 40, 50 and 70% were obtained by adding a portion of dry N<sub>2</sub> followed by bubbling N<sub>2</sub> (100% humid) through a fritted glass immersed in water to give a total pressure of 1 atm. Gaseous reactants and products in the long path cell were measured using FTIR starting immediately after the addition of the reactants, for up to 350 min reaction time. Loss of NO and formation of gaseous NO<sub>2</sub> and HONO were measured using their absorption bands at 1876, 2900, and 1264 cm<sup>-1</sup>, respectively.

Spectra of these species were quantitatively analyzed using a least-squares fitting procedure described in detail by Gomer et al.<sup>28</sup> The concentration of each species is determined relative to a reference spectrum of known concentration. Absolute concentrations for NO and NO<sub>2</sub> reference spectra were determined using calibrations of the pure gases. Nitrous acid was quantified using infrared cross sections for 1264 cm<sup>-1</sup> peak determined by Barney et al.<sup>29,30</sup> in this laboratory.

**Materials.** HNO<sub>3</sub> was 70.1 wt % (Fisher) and H<sub>2</sub>SO<sub>4</sub> was 95.8 wt % (Fisher). Nitric oxide (Matheson 99%) was purified by passing it rapidly through a liquid nitrogen trap. The N<sub>2</sub> was 99.999% (Oxygen Services Company) and used as received.

## III. Results and Discussion

**A. Water Coverage on Glass.** Figure 2a shows typical infrared spectra in the 3800 to 2800 cm<sup>-1</sup> region where absorptions due to the stretching vibrations of water occur. The

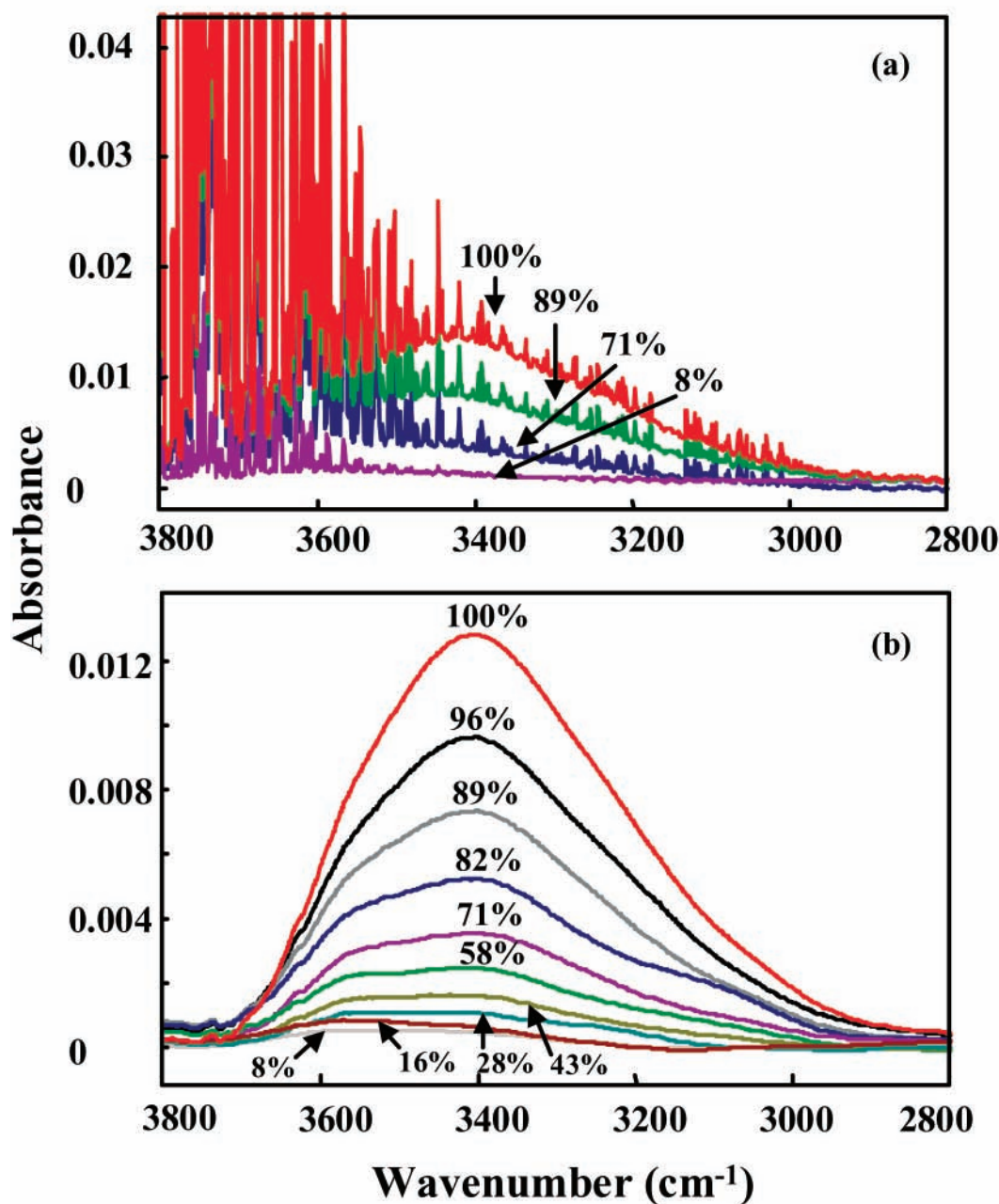


**Figure 2.** (a) Typical absorption spectra of water adsorbed on thin cover glass disks at different relative humidities and at room temperature; (b) spectra from (a) plotted at lower resolution ( $4\text{ cm}^{-1}$ ) with gas-phase water subtracted and smoothing of the spectra.

$\nu_1$  stretch of gas-phase water is centered at  $3652\text{ cm}^{-1}$  and the asymmetric  $\nu_3$  stretch at  $3756\text{ cm}^{-1}$ .<sup>31</sup> These bands appear as a series of sharp rotational lines superimposed on a broad band centered at  $\sim 3400\text{ cm}^{-1}$  at the highest water coverages. The broad band is due to liquid water, and is red-shifted by up to 200 wavenumbers compared to the gas phase due to intermolecular hydrogen bonding;<sup>32</sup> the shift in band position from the gas to the liquid is also accompanied by an increase in the absorption coefficient.<sup>32</sup>

Figure 2b shows more clearly the surface water band. These spectra were obtained by subtracting from Figure 2a the contribution from gas-phase water, converting the spectra to a lower resolution ( $4\text{ cm}^{-1}$  instead of  $0.5\text{ cm}^{-1}$  which is adequate for this broad band), and smoothing them. These show that the surface water peak shifts from  $\sim 3600\text{ cm}^{-1}$  to  $\sim 3400\text{ cm}^{-1}$  as the water coverage increases, and at 100% RH, the spectrum becomes indistinguishable from that of liquid water. The shift

toward lower wavenumbers in the presence of more surface water reflects a trend in which water changes from strong interactions with the surface with some hydrogen-bonding to adjacent water molecules, to three-dimensional water hydrogen-bonding as is the case of the bulk liquid. This is similar to the effects observed by Ewing and co-workers<sup>33,34</sup> on the infrared spectrum of water adsorbed on NaCl crystals, in which the center of the  $3400\text{ cm}^{-1}$  band was red-shifted to  $3500\text{ cm}^{-1}$  at submonolayer coverages.

The number of monolayers ( $ML$ ) of adsorbed  $\text{H}_2\text{O}$  on glass as a function of relative humidity was calculated from the integrated absorbance,  $\tilde{A}$  ( $\text{cm}^{-1}$ ), and the known integrated absorption coefficient for liquid water,<sup>33–35</sup>  $\bar{\sigma} = 6.1 \times 10^{-17}\text{ cm molecule}^{-1}$  (base 10)

$$ML = \tilde{A} / (1.0 \times 10^{15} N \bar{\sigma}) \quad (1)$$

where  $N = 10$  is the number of thin cover glass surfaces and



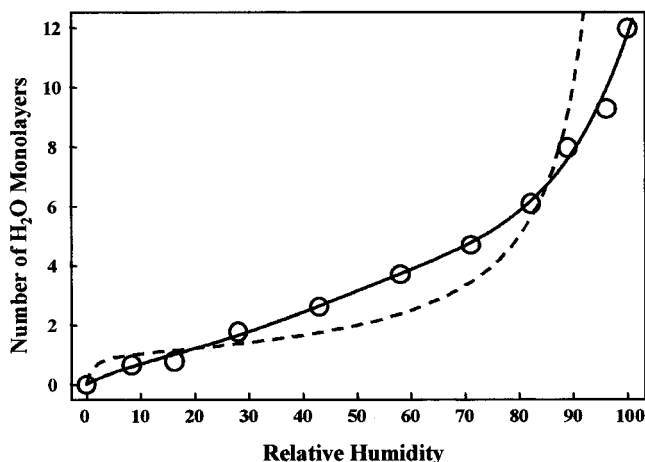


**Figure 3.** Number of monolayers of adsorbed H<sub>2</sub>O on cover glass as a function of relative humidity. The solid line is a fit to the data and the dotted line shows a BET isotherm for multilayer adsorption.

$1 \times 10^{15}$  molecule cm<sup>-2</sup> is the surface density of one monolayer of water, based on an area per water molecule of  $10 \text{ \AA}^2$ .<sup>36</sup> An integrated absorption coefficient of  $\bar{\sigma} = 6.1 \times 10^{-17}$  cm molecule<sup>-1</sup> was used for all water coverages on the surface. In order to avoid systematic errors in determining the number of water layers that might be introduced by the smoothing procedure, the spectra used for quantification were the  $0.5 \text{ cm}^{-1}$  spectra (Figure 2a) but with the contribution of gas-phase water subtracted out. Figure 2 shows the blue shift in the absorption spectrum due to a strong interaction between water and the surface at low coverages; it is therefore expected that the absorption coefficient will also be smaller than that for bulk liquid water at these lower coverages. However, given the uncertainty inherent in estimating the correction factor for the absorption coefficient for such a perturbed liquid-surface system, we have used the bulk liquid water value at all coverages.

Figure 3 summarizes the number of monolayers of water on the glass surface as a function of the relative humidity. The data suggest a Type II isotherm<sup>37</sup> characteristic of multilayer adsorption. The dotted line shown in Figure 3 represents a fit for a BET isotherm of the form<sup>37</sup>

$$\text{fractional coverage} = \frac{c_B RH}{(1 - RH)[1 + (c_B - 1)RH]} \quad (\text{II})$$

where  $c_B = 100$  is a constant. We understand that although the fit could be improved with a multi-parameter model, the data in Figure 3 are adequate for determining the number of water layers under our experimental conditions.

Our data are consistent with literature reports of the uptake of water on glass,<sup>38</sup> particularly given the different analytical methods that were used and the different treatments under which the glass surfaces were prepared. It is interesting, for example, to note that in 1918 Langmuir reported that 4.5 layers of water were adsorbed on glass in air.<sup>39</sup> This would be consistent with ~70% RH in their laboratory.

There is a great deal of evidence that the first few layers of water on silica surfaces interact strongly with the surface and do not behave like bulk liquid water. At least the first three layers of water are known to be strongly perturbed.<sup>40–42</sup> In addition, water is known to form clusters on the surface at low coverages, rather than forming a uniform thin film.<sup>40–43</sup> As a result, in our experimental system, the water on the surface is better thought of as clusters at relative humidities at or below 50%. Therefore, one, two or three layers of water on the surface

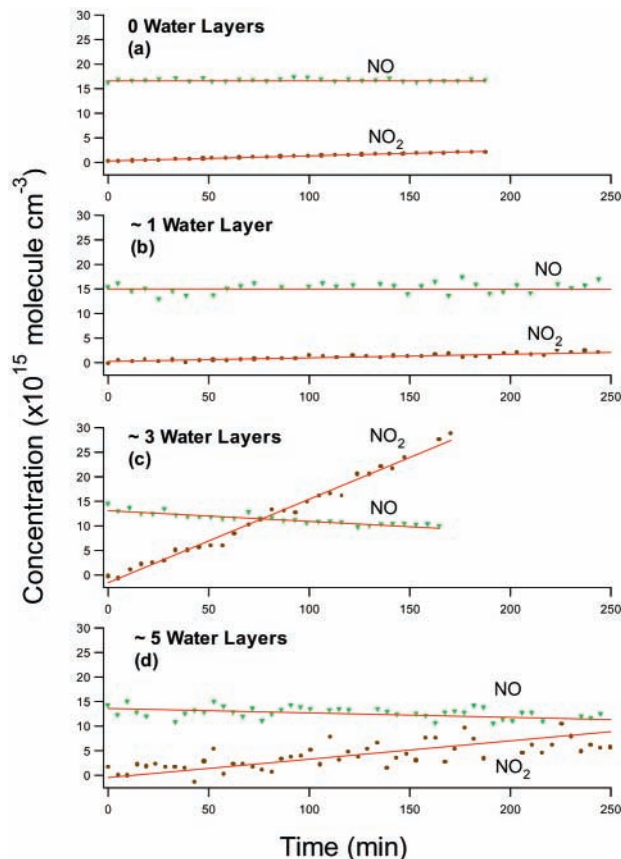


**Figure 4.** Decay of gas-phase NO and formation of NO<sub>2</sub> in the long path cell whose walls had first been exposed to HNO<sub>3</sub>. (a) 0% RH and [NO]<sub>0</sub> =  $1.6 \times 10^{16}$  molecule cm<sup>-3</sup> (b) 30% RH and [NO]<sub>0</sub> =  $1.4 \times 10^{16}$  molecule cm<sup>-3</sup>; (c) 50% RH and [NO]<sub>0</sub> =  $1.4 \times 10^{16}$  molecule cm<sup>-3</sup>; (d) 70% RH and [NO]<sub>0</sub> =  $1.4 \times 10^{16}$  molecule cm<sup>-3</sup>. The total pressure was 1 atm in N<sub>2</sub> at room temperature.

are used in the context of “equivalent numbers of layers” because the water is unevenly distributed.

We assume in the experiments with HNO<sub>3</sub> on the surface that preadsorbing HNO<sub>3</sub> on the glass does not alter the subsequent uptake of water. Although Bogdan and Kulmala<sup>44</sup> reported that HNO<sub>3</sub> and HCl do affect the uptake of water on silica powder, we did not observe an increase in the  $5275 \text{ cm}^{-1}$  combination infrared band of water on silica powder when it had been “dosed” with HNO<sub>3</sub> before exposure to water vapor.<sup>45</sup> (This band was followed to avoid interfering absorptions in the  $3000\text{--}3500 \text{ cm}^{-1}$  region by HNO<sub>3</sub> itself).

**B. Reaction of Gaseous NO with HNO<sub>3</sub>–H<sub>2</sub>O Thin Surface Films.** Figure 4a shows the results of a typical experiment in which a mixture of NO in N<sub>2</sub> was added to the cell in the absence of water after dosing with HNO<sub>3</sub>. There was no detectable loss of NO and only a slow formation of NO<sub>2</sub>. This could be due to some thermal oxidation of NO by molecular oxygen impurities from small amounts of air leakage into the cell during these long experiments, or to a very slow reaction between NO and HNO<sub>3</sub> on the cell surface. With approximately one monolayer of water, a slightly higher rate of NO<sub>2</sub> formation was observed (e.g., Figure 4b). With three monolayers of water, the reaction was much faster, with measurable losses of NO and rapid formation of NO<sub>2</sub> (e.g., Figure 4c). However, with a further increase in water coverage to five layers (Figure 4d), the rate of formation of NO<sub>2</sub> again decreased.

The stoichiometry  $\Delta[\text{NO}_2]/\Delta[\text{NO}]$  was calculated from the slopes of the lines obtained when NO and NO<sub>2</sub> were plotted as

**TABLE 1: Summary of Long Path Cell FTIR Measurements of the Decay of NO and Formation of NO<sub>2</sub> in the Reaction of NO with HNO<sub>3</sub> Adsorbed on the Cell Walls at Different Water Coverages on the Surface**

number of surface water layers (%RH)	experiment #	[NO] <sub>0</sub> (10 <sup>15</sup> molecule cm <sup>-3</sup> )	-d[NO]/dt (10 <sup>13</sup> molecule cm <sup>-3</sup> min <sup>-1</sup> )	d[NO <sub>2</sub> ]/dt (10 <sup>13</sup> molecule cm <sup>-3</sup> min <sup>-1</sup> )	ΔNO <sub>2</sub> /ΔNO <sup>a</sup>	average ± 2σ
1.9 (30)	1	4.0	0.12	0.35	2.9	3.8 ± 1.1
	2	7.2	0.14	0.47	3.3	
	3	9.5	0.46	2.5	5.4	
	4	15.0	0.63	2.2	3.5	
2.5 (40)	1	2.6	0.08	0.2	2.5	3.2 ± 0.6
	2	8.0	0.42	1.5	3.6	
	3	11.0	0.59	2.2	3.7	
	4	15.0	1.1	3.3	3.0	
3 (50)	1	0.65	0.095	0.35	3.7	3.3 ± 0.4
	2	3.2	0.36	1.1	3.0	
	3	7.0	0.91	2.6	2.8	
	4	8.2	2.0	7.1	3.6	
	5	14	4.3	15	3.5	
	6	22	7.3	20	2.7	
	7	40	11	40	3.6	

<sup>a</sup> From the ratio of {d[NO<sub>2</sub>]/dt}/{d[NO]/dt}.

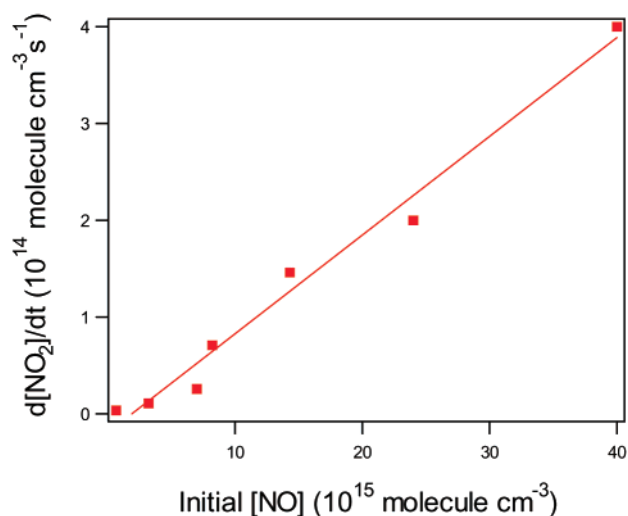


**Figure 5.** Rate of NO<sub>2</sub> formation as a function of initial NO concentration at 1 atm pressure in N<sub>2</sub> and 50% RH.

a function of time between 0 and 300 min for the runs where 2–3 layers of water were on the surface. Table 1 summarizes these data. The weighted average is  $\Delta[\text{NO}_2]/\Delta[\text{NO}] = 3.3 \pm 1.0$  ( $2\sigma$ ). Small concentrations of HONO ( $\sim 10^{14}$  molecule cm<sup>-3</sup>) were detected at larger reaction times; for example, with an initial NO concentration of  $2.2 \times 10^{16}$  molecule cm<sup>-3</sup> and three layers of surface water, HONO at 260 min was  $\sim 2 \times 10^{14}$  molecule cm<sup>-3</sup> compared to NO<sub>2</sub> at  $4 \times 10^{16}$  molecule cm<sup>-3</sup>. Because HONO was detectable when significant amounts of NO<sub>2</sub> had been formed, it may have been generated at least in part by the surface NO<sub>2</sub> hydrolysis reaction.<sup>2–16</sup>

Figure 5 shows the rate of NO<sub>2</sub> formation in the long path cell as a function of the initial NO concentrations under conditions where three layers of surface water were present, indicating that the reaction generating NO<sub>2</sub> is first-order in NO.

To ensure that NO<sub>2</sub> formation was due to reaction 5, blank runs were also carried out in which NO was introduced alone into the clean cell whose walls had been cleaned by rinsing with Nanopure water. Spectra of NO in the cell at 0 and 50% RH were collected as a function of time; no significant formation of NO<sub>2</sub> was observed. Similarly, blank runs in which nitric acid alone was introduced into the cell at various RH also gave no reaction.

These experiments clearly show that the rate of the heterogeneous reaction of gaseous NO with HNO<sub>3</sub> on borosilicate glass depends strongly on the presence of water on the surface. The reaction was so slow as to be undetectable in the absence of water, but accelerated as the number of surface water layers approached three. With further increases in water, however, the rate again decreased.

Nitric acid is expected to hydrogen bond with the polar silanol groups (–Si–OH) at the silica surface.<sup>40,46,47</sup> Independent evidence for this HNO<sub>3</sub>–silica interaction was obtained<sup>45</sup> from the absorption spectrum of porous glass and silica before and after dosing with HNO<sub>3</sub>. The sharp peak at  $\sim 3750$  cm<sup>-1</sup> due to the O–H stretch of free (i.e., not hydrogen-bonded) –SiOH surface groups<sup>32</sup> decreased upon adsorption of HNO<sub>3</sub> but recovered when HNO<sub>3</sub> was removed by extensive pumping. Thus, we attribute the decrease in the peak to a reversible hydrogen-bonding of HNO<sub>3</sub> to the silanol group. A similar change has been observed by Goodman et al.<sup>21</sup> when silica powders were exposed to gaseous HNO<sub>3</sub>. The strength of this hydrogen-bond can be estimated from ab initio calculations by Tao et al.<sup>48</sup> of the binding of nitric acid to water in the gas phase. The binding energy was estimated to be  $\sim 30$  kJ mol<sup>-1</sup>, with two hydrogen bonds formed between the molecules. A reasonable value for one hydrogen bond between water and nitric acid is therefore 15 kJ mol<sup>-1</sup>, which lies in the range of 12–24 kJ mol<sup>-1</sup> reported for a variety of hydrogen bonds.<sup>32</sup>

When small amounts of water are adsorbed on silica surfaces, it is believed to cluster on the surface rather than forming a uniformly distributed layer. This is attributed to an enthalpy of adsorption of water on water clusters that is greater than that for adsorption on an isolated silanol group (44 kJ mol<sup>-1</sup> vs 25 kJ mol<sup>-1</sup>).<sup>40</sup> When nitric acid has been preadsorbed on the surface as in these experiments, water may cluster around the surface HNO<sub>3</sub>. An alternate possibility is that water displaces HNO<sub>3</sub> from the silanol group onto the adjacent surface, but that HNO<sub>3</sub> remains in close proximity to the water now clustered around the –SiOH group; the latter is suggested by the greater strength of the hydrogen bond between water and the –SiOH group (25 kJ mol<sup>-1</sup>) compared to that between nitric acid and water, estimated to be  $\sim 15$  kJ mol<sup>-1</sup>. When both water and nitric acid are present, water stabilizes HNO<sub>3</sub> by as much as 30 kJ mol<sup>-1</sup> relative to the gas phase, assuming two hydrogen-bonds to nitric acid are involved.

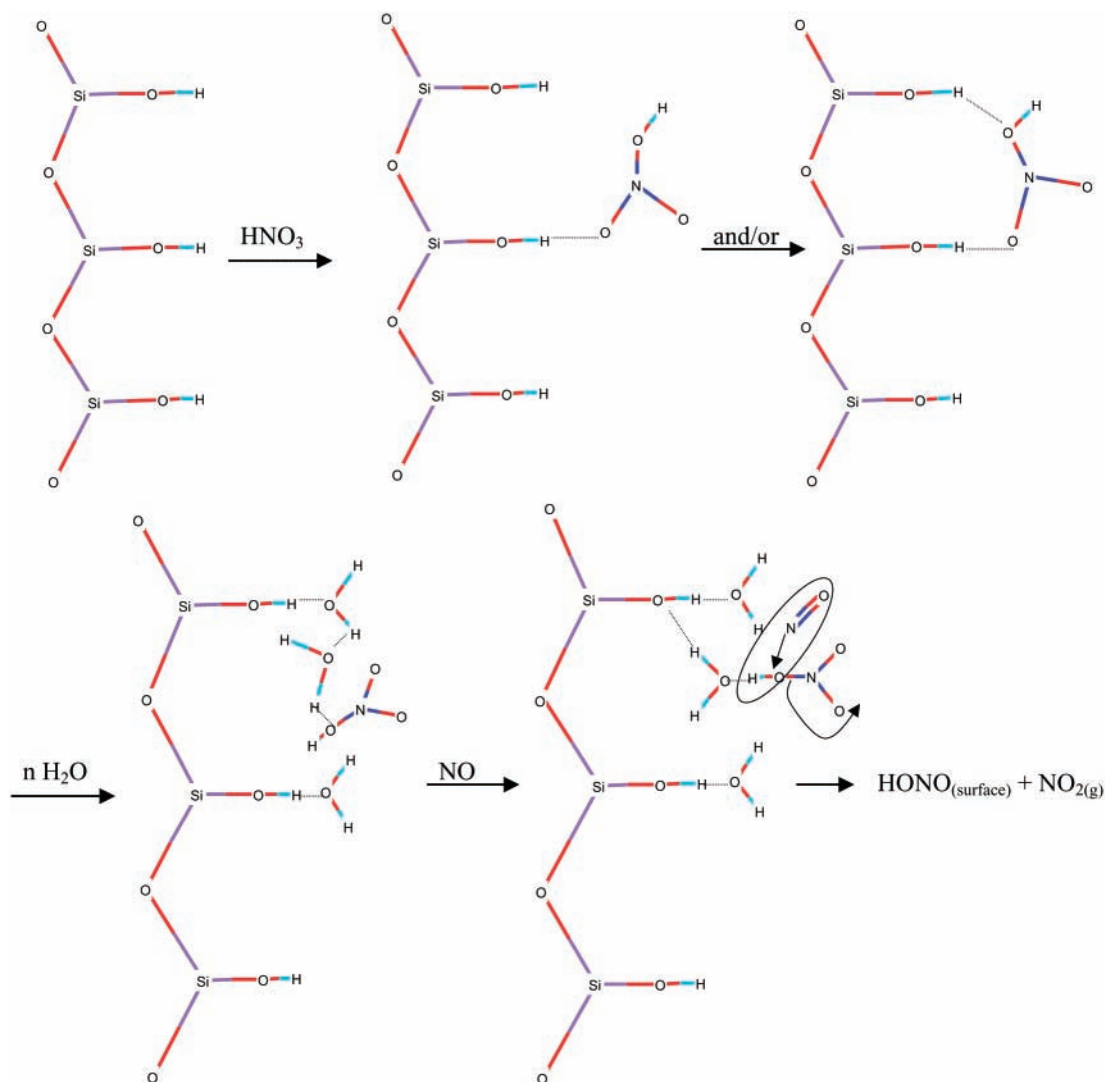


**Figure 6.** Model of reaction of  $\text{HNO}_3$  with  $\text{NO}$  on a silica surface in the presence of water.

It is relevant that  $\text{HNO}_3$  readily desorbs back into the gas phase in a dry cell but most of it remains on the surface where water is present. In a dry cell, the amount of  $\text{HNO}_3$  desorbing into the gas-phase varies, depending on the condition of the cell walls. A typical peak absorbance of  $\sim 0.3\text{--}0.6$  at  $896\text{ cm}^{-1}$  is observed after dosing  $\text{HNO}_3$  in a dry cell, compared to  $\sim 0.1$  after water vapor is added. Figure 6 summarizes this model of nitric acid and water on the surface.

Gaseous  $\text{NO}$  introduced in the cell reacts with the adsorbed  $\text{HNO}_3$  surrounded by water molecules to produce  $\text{NO}_2$  and  $\text{HONO}$



If the reactants and products in reaction 2 are in the gas phase, the standard enthalpy of reaction is  $\Delta H_{298\text{K}}^0 = -1.4\text{ kJ mol}^{-1}$ . However, our experiments show that in order for reaction 2 to occur, (i)  $\text{HNO}_3$  must be on the surface, and (ii) water must be present. As discussed above, nitric acid hydrogen-bonded to the surface and to a water molecule is estimated to be stabilized compared to the gas phase<sup>32</sup> by  $\sim 30\text{ kJ mol}^{-1}$ , making the reaction endothermic by  $\sim 29\text{ kJ mol}^{-1}$ .

However, water is also capable of solvating the reaction products. The Henry's Law constants,  $49\text{ L mol}^{-1}\text{ atm}^{-1}$  for  $\text{HONO}$  compared to  $1.4 \times 10^{-2}$  for  $\text{NO}_2$ ,<sup>19,49</sup> show that nitrous acid interacts more strongly with water than does  $\text{NO}_2$ , and

hence, solvation of  $\text{HONO}$  as it is formed should be particularly important. The difference between the enthalpy of formation<sup>50</sup> of  $\text{HONO}$  in the gas phase compared to solution (undissociated  $\text{HONO}$ ) is  $40\text{ kJ mol}^{-1}$ . This is more than sufficient to make the reaction between  $\text{NO}$  and surface hydrogen-bonded  $\text{HNO}_3$  exothermic. The product  $\text{NO}_2$  will be formed initially in the water cluster and solvation of this product will further increase the reaction exothermicity. Because  $\text{NO}_2$  is much less soluble, it will be released to the gas phase as shown in Figure 6, whereas  $\text{HONO}$  remains on the surface to undergo further reaction with adsorbed nitric acid.

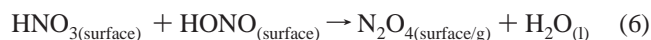
As discussed earlier, the subsequent chemistry of  $\text{HONO}$  on the surface may either be the reaction with another surface  $\text{HNO}_3$  or the bimolecular reaction between two  $\text{HONO}$  molecules on the surface. Although neither can be firmly ruled out based on our experiments, the former seems more likely



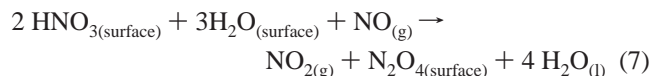
The enthalpy of this gas-phase reaction is  $\Delta H_{298\text{K}}^0 = +39\text{ kJ mol}^{-1}$ . Assuming, as discussed previously, that  $\text{HNO}_3$  is stabilized by  $30\text{ kJ mol}^{-1}$ ,  $\text{HONO}$  is stabilized by  $40\text{ kJ mol}^{-1}$  due to solvation, and the water is generated in the liquid state, the reaction enthalpy becomes  $+65\text{ kJ mol}^{-1}$ . However, it is mechanistically reasonable to suggest that the  $\text{HONO} - \text{HNO}_3$  reaction initially generates  $\text{N}_2\text{O}_4$  rather than  $2\text{NO}_2$ , and the



reaction then becomes



If the  $\text{N}_2\text{O}_4$  product is in the gas phase, the standard enthalpy change for reaction 4 becomes  $+8 \text{ kJ mol}^{-1}$ . However, solvation of  $\text{N}_2\text{O}_4$  as it is formed will stabilize this product, increasing the reaction exothermicity.  $\text{N}_2\text{O}_4$  is much more soluble than  $\text{NO}_2$  in water, with its Henry's Law constant<sup>19</sup> being 2 orders of magnitude larger than that for  $\text{NO}_2$ . As an upper limit, we estimate an additional gain of  $29 \text{ kJ mol}^{-1}$  based on the difference between gaseous and liquid  $\text{N}_2\text{O}_4$ . Dissociation of  $\text{N}_2\text{O}_4$  then releases  $\text{NO}_2$  into the gas phase. Given the critical role played by water, the most accurate representation of the overall reaction may be



This model is consistent with the work of Bogdan and co-workers<sup>44,51,52</sup> who studied the uptake of nitric acid and water on silica powders. They reported that the concentration of nitric acid was larger in the layers adjacent to the silica surface<sup>51</sup> and that the enthalpies of fusion of microdroplets of nitric acid and water on these surfaces are lower than for the bulk acid–water solutions.<sup>52</sup> Thus, nitric acid and water on silica surfaces cannot be treated as bulk aqueous systems.

The reaction with five layers of water present on the surface (Figure 4) is much slower than that with two to three layers of water. This is likely due to the fact that water behaves like a bulk liquid at these higher coverages.<sup>40–42</sup> Thus, under these conditions the surface water may more closely resemble a bulk aqueous solution of nitric acid, rather than surface-adsorbed clusters as proposed in the model in Figure 6. Nitric acid is well-known to dissociate in dilute aqueous solutions, even on surfaces. Supporting this possibility is the observation by Goodman et al.<sup>21</sup> and by this laboratory<sup>45</sup> that addition of water vapor at high relative humidities when  $\text{HNO}_3$  is adsorbed on silica leads to a decrease in the molecular nitric acid peak and an increase in nitrate ion peaks. At the other extreme, if the film is highly concentrated in nitric acid, molecular  $\text{HNO}_3$  associates with water molecules to form hydrates.<sup>53–59</sup> Under these conditions, the vapor pressure of nitric acid in equilibrium with the solution is quite high (of the order of Torr)<sup>56</sup> and less nitric acid may remain on the silica surface for reaction.

**Atmospheric Implications.** Silica surfaces are ubiquitous in the troposphere in the form of dust particles, soil and building materials. Nitric acid is well-known to be readily taken up by such surfaces.<sup>19–22</sup> The studies presented here suggest that the sticking of nitric acid to such surfaces is more efficient in the presence of surface water; given that water vapor is always present in the lower atmosphere, this will not be a limiting factor under atmospheric conditions. Our studies show that with the appropriate amount of water on the surface,  $\text{HNO}_3$  can potentially be converted into  $\text{NO}_2$ . Such “renoxification” has significant implications for the chemistry of both the free troposphere and polluted urban areas. In order for such chemistry to occur, there must be sufficient water on the surface to stabilize the  $\text{HNO}_3$  and to solvate the reaction products. On the other hand, if there is so much water on the surface that it behaves like a bulk liquid and the nitric acid is largely dissociated, the reaction does not occur. The data presented here with approximately three surface monolayers of water imply that the reaction probability for loss of  $\text{NO}$  on the cell walls under these conditions is of the order of  $10^{-8}$ . However, this cannot be

directly applied to the atmosphere because the actual form of nitric acid on the cell walls and how that relates to atmospheric conditions is not known. Understanding the amounts of water on surfaces in the lower atmosphere and the form of surface nitric acid are key to assessing the importance of this chemistry under various atmospheric conditions. Increased reactive surface areas of soils<sup>60</sup> compared to the geometric surface area at the earth's surface must also be taken into account. Finally, the reaction kinetics of  $\text{NO}$  with the nitric acid–water clusters needs to be directly assessed. Such studies are currently underway in this laboratory.

#### IV. Conclusions

Gaseous nitric oxide reacts at room temperature with nitric acid on a glass surface in the presence of water. The major gaseous product is  $\text{NO}_2$ , with the overall reaction stoichiometry corresponding to 3  $\text{NO}_2$  produced per  $\text{NO}$  reacted. The reaction is first order with respect to  $\text{NO}$ . These experimental observations are consistent with the overall reaction  $2 \text{HNO}_{3(\text{surface})} + \text{NO}_{(\text{g})} \rightarrow 3 \text{NO}_{2(\text{g})} + \text{H}_2\text{O}_{(\text{l})}$ . However, the presence of water on the surface is critical. Its role is likely to solvate the  $\text{HNO}_3$  and  $\text{N}_2\text{O}_4$  products generated in two steps that make up the overall reaction. We propose a model in which  $\text{HNO}_3$  is hydrogen-bonded to the surface in close proximity to water. As a result, the overall reaction may be better represented as follows:  $2 \text{HNO}_{3(\text{surface})} + 3\text{H}_2\text{O}_{(\text{surface})} + \text{NO}_{(\text{g})} \rightarrow \text{NO}_{2(\text{g})} + \text{N}_2\text{O}_{4(\text{surface})} + 4 \text{H}_2\text{O}_{(\text{l})}$ . This chemistry is potentially important in “renoxification” of  $\text{HNO}_3$  in the boundary layer of polluted urban atmospheres where silica surfaces are plentiful in particles, soils and building materials, as well as globally in the free troposphere where dust particles are present.

**Acknowledgment.** We are grateful to the California Air Resources Board for support of this work. We also thank J. N. Pitts, Jr. for helpful discussions and encouragement to study these heterogeneous systems, V. H. Grassian, G. E. Ewing, D. Tobias and P. Jungwirth for providing preprints prior to publication and for helpful discussions, and J. Meyer for technical assistance.

#### References and Notes

- (1) Smith, J. H. *J. Am. Chem. Soc.* **1947**, *69*, 1741.
- (2) Goodman, A. L.; Underwood, G. M.; Grassian, V. H. *J. Phys. Chem. A* **1999**, *103*, 7217.
- (3) Barney, W. S.; Finlayson-Pitts, B. J. *J. Phys. Chem. A* **2000**, *104*, 171.
- (4) Sakamaki, F.; Hatakeyama, S.; Akimoto, H. *Int. J. Chem. Kinet.* **1983**, *15*, 1013.
- (5) Pitts, J. N.; Sanhueza, E.; Atkinson, R.; Carter, W. P. L.; Winer, A. M.; Harris, G. W.; Plum, C. N. *Int. J. Chem. Kinet.* **1984**, *16*, 919.
- (6) Svensson, R.; Ljungstrom, E.; Lindqvist, O. *Atmos. Environ.* **1987**, *21*, 1529.
- (7) Jenkin, M. E.; Cox, R. A.; Williams, D. J. *Atmos. Environ.* **1988**, *22*, 487.
- (8) Febo, A.; Perrino, C. *Atmos. Environ.* **1991**, *25A*, 1055.
- (9) Bambauer, A.; Brantner, B.; Paige, M.; Novakov, T. *Atmos. Environ.* **1994**, *28*, 3225.
- (10) Mertes, S.; Wahner, A. *J. Phys. Chem.* **1995**, *99*, 14 000.
- (11) Harrison, R. M.; Peak, J. D.; Collins, G. M. *J. Geophys. Res.* **1996**, *101*, 14 429.
- (12) Lammel, G.; Cape, J. N. *Chem. Soc. Rev.* **1996**, *25*, 361.
- (13) Kleffmann, J.; Becker, K. H.; Wiesen, P. *Atmos. Environ.* **1998**, *32*, 2721.
- (14) Kleffmann, J.; Becker, K. H.; Wiesen, P. *J. Chem. Soc., Faraday Trans.* **1998**, *94*, 3289.
- (15) Harrison, R. M.; Collins, G. M. *J. Atmos. Chem.* **1998**, *30*, 397.
- (16) Wingen, L.; Yang, H.; Sumner, A. L.; Finlayson-Pitts, B. J., in preparation, **2001**.

- (17) Mochida, M.; Finlayson-Pitts, B. J. *J. Phys. Chem. A* **2000**, *104*, 9705.
- (18) Fairbrother, D. H.; Sullivan, D. J. D.; Johnston, H. S. *J. Phys. Chem. A* **1997**, *101*, 7350.
- (19) Finlayson-Pitts, B. J.; Pitts, J. N. *Chemistry of the Upper and Lower Atmosphere: Theory, Experiments and Applications*; Academic Press: New York, 2000.
- (20) Padgett, P. E.; Bytnerowicz, A. *Atmos. Environ.* **2001**, *35*, 2405.
- (21) Goodman, A. L.; Bernard, E. T.; Grassian, V. H. *J. Phys. Chem. A* **2001**, *105*, 6443.
- (22) Hanisch, F.; Crowley, J. N. *J. Phys. Chem. A* **2001**, *105*, 3096.
- (23) Dentener, F. J.; Carmichael, G. R.; Zhang, Y.; Lelieveld, J.; Crutzen, P. J. *J. Geophys. Res.* **1996**, *101*, 22.
- (24) Underwood, G. M.; Song, C. H.; Phadnis, M.; Carmichael, G. R.; Grassian, V. H. *J. Geophys. Res.* **2001**, *106*, 18055.
- (25) Chatfield, R. B. *Geophys. Res. Lett.* **1994**, *21*, 2705.
- (26) Hauglustaine, D. A.; Ridley, B. A.; Solomon, S.; Hess, P. G.; Madronich, S. *Geophys. Res. Lett.* **1996**, *23*, 2609.
- (27) Lary, D. J.; Lee, A. M.; Toumi, R.; Newchurch, M. J.; Pirre, M.; Renard, J. B. *J. Geophys. Res.* **1997**, *102*, 3671.
- (28) Gomer, T.; Brauers, T.; Heintz, F.; Stutz, J.; Platt, U. *University of Heidelberg* 1995.
- (29) Barney, W. S.; Wingen, L. M.; Lakin, M. J.; Brauers, T.; Stutz, J.; Finlayson-Pitts, B. J. *J. Phys. Chem. A* **2000**, *104*, 1692.
- (30) Barney, W. S.; Wingen, L. M.; Lakin, M. J.; Brauers, T.; Stutz, J.; Finlayson-Pitts, B. J. *J. Phys. Chem. A* **2001**, *105*, 4166.
- (31) Herzberg, G. *Molecular Spectra and Molecular Structure. II. Infrared and Raman Spectra of Polyatomic Molecules*; D. Van Nostrand Company, Inc.: Princeton, N. J., 1945; Vol. II.
- (32) Pimentel, G. C.; McClellan, A. L. *The Hydrogen Bond*; W. H. Freeman: San Francisco, 1960.
- (33) Foster, M.; Ewing, G. E. *Surf. Sci.* **1999**, *427/428*, 102.
- (34) Foster, M. C.; Ewing, G. E. *J. Chem. Phys.* **2000**, *112*, 6817.
- (35) Weis, D. D.; Ewing, G. E. *J. Geophys. Res.* **1996**, *101*, 18 709.
- (36) Chattoraj, D. K.; Birdi, K. S. *Adsorption and the Gibbs Surface Excess*; Plenum Press: New York, 1984.
- (37) Masel, R. I. *Principles of Adsorption and Reaction on Solid Surfaces*; Wiley: New York, 1996.
- (38) Frazer, J. H. *Phys. Rev.* **1929**, *33*, 97.
- (39) Langmuir, I. *J. Am. Chem. Soc.* **1918**, *40*, 1361.
- (40) Iler, R. K. *The Chemistry of Silica*; Wiley: New York, 1978.
- (41) Icenhower, J. P.; Dove, P. M. Water Behaviour at Silica Surfaces. In *Adsorption on Silica Surfaces*; Papirer, E., Ed.; Marcel Dekker: New York, 2000; Ch. 9.
- (42) *Adsorption on Silica Surfaces*; Papirer, E., Ed.; Marcel Dekker: New York, 2000; Vol. 90.
- (43) Bogdan, A. Fumed Silica as a Host for Study of the Large Surface-to-Volume Ratio Problems in Finely Divided Aqueous Systems: Implications for the Atmosphere. In *Adsorption on Silica Surfaces*; Papirer, E., Ed.; Marcel Dekker: New York, 2000.
- (44) Bogdan, A.; Kulmala, M. *J. Colloid Interfac. Sci.* **1997**, *191*, 95.
- (45) Sumner, A. L.; Ramazan, K.; Rivera, A.; Finlayson-Pitts, B. J. **2001**, unpublished results.
- (46) Chuang, I.-S.; Kinney, D. R.; Bronnimann, C. E.; Ziegler, R. C.; Maciel, G. E. *J. Phys. Chem.* **1992**, *96*, 4027.
- (47) Bronnimann, C. E.; Zeigler, R. C.; Maciel, G. E. *J. Am. Chem. Soc.* **1988**, *110*, 2023.
- (48) Tao, F.-M.; Higgins, K.; Klemperer, W.; Nelson, D. D. *Geophys. Res. Lett.* **1996**, *23*, 1797.
- (49) Cheung, J. L.; Li, Y. Q.; Boniface, J.; Shi, Q.; Davidovits, P.; Worsnop, D. R.; Jayne, J. T.; Kolb, C. E. *J. Phys. Chem. A* **2000**, *104*, 2655.
- (50) Wagman, D. D.; Evans, W. H.; Parker, V. B.; Schumm, R. H.; Halow, I.; Balley, S. M.; Churney, K. L.; Nuttall, R. L. *J. Phys. Chem. Ref. Data* **1982**, *11*, Suppl. No. 2.
- (51) Bogdan, A.; Kulmala, M.; Gorbunov, B.; Kruppa, A. *J. Colloid Interfac. Sci.* **1996**, *177*, 79.
- (52) Bogdan, A.; Kulmala, M. *Geophys. Res. Lett.* **1999**, *26*, 1433.
- (53) Redlich, O.; Bigeleisen, J. *J. Am. Chem. Soc.* **1943**, *65*, 1883.
- (54) Redlich, O. *Chem. Rev.* **1946**, *39*, 333.
- (55) Miles, F. D. *Nitric Acid Manufacture and Uses*; Oxford University Press: London, 1961.
- (56) Davis, W. J.; DeBruin, H. J. *J. Inorg. Nucl. Chem.* **1964**, *26*, 1069.
- (57) Schwartz, S. E.; White, W. H. Solubility Equilibria of the Nitrogen Oxides and Oxyacids in Dilute Aqueous Solution. In *Advances in Environmental Science and Engineering*; Pfafflin, J. R., Ziegler, E. N., Eds.; Gordon and Breach Science Publishers: New York, 1981; Vol. 4; p 1.
- (58) Koller, J.; Hazdi, D. *J. Mol. Structure* **1991**, *247*, 225.
- (59) Molina, M. J.; Zhang, R.; Wooldridge, P. J.; McMahon, J. R.; Kim, J. E.; Chang, H. Y.; Beyers, K. D. *Science* **1993**, *261*, 1418.
- (60) Hodson, M. E.; Langan, S. J.; Kennedy, F. M.; Bain, D. C. *Geoderma* **1998**, *85*, 1.